MATEC Web of Conferences **16**, 04001 (2014)
DOI: 10.1051/matecconf/20141604001

Jump and pull-in dynamics of an electrically actuated bistable MEMS device

Laura Ruzziconi[1], Stefano Lenci[1], and Mohammad I. Younis[2,3]

[1] Department of Civil and Building Engineering and Architecture, Polytechnic University of Marche, via Brecce Bianche, 60131 Ancona, Italy
[2] Physical Sciences and Engineering Division, King Abdullah University of Science and Technology (KAUST), Thuwal 23955-6900, Kingdom of Saudi Arabia
[3] Department of Mechanical Engineering, State University of New York at Binghamton, Binghamton, 13902 NY, USA
Emails: l.ruzziconi@univpm.it, lenci@univpm.it, mohammad.younis@kaust.edu.sa and myounis@binghamton.edu

Abstract. This study analyzes a theoretical bistable MEMS device, which exhibits a considerable versatility of behavior. After exploring the coexistence of attractors, we focus on each rest position, and investigate the final outcome, when the electrodynamic voltage is suddenly applied. Our aim is to describe the parameter range where each attractor may practically be observed under realistic conditions, when an electric load is suddenly applied. Since disturbances are inevitably encountered in experiments and practice, a dynamical integrity analysis is performed in order to take them into account. We build the integrity charts, which examine the practical vulnerability of each attractor. A small integrity enhances the sensitivity of the system to disturbances, leading in practice either to jump or to dynamic pull-in. Accordingly, the parameter range where the device, subjected to a suddenly applied load, can operate in safe conditions with a certain attractor is smaller, and sometimes considerably smaller, than in the theoretical predictions. While we refer to a particular case-study, the approach is very general.

1 Introduction

Complex nonlinear features represent a very attractive opportunity for improving performances of micro- and nano-systems [1, 2]. New sophisticated devices deliberately operating in the nonlinear regime are emerging in a variety of different applications, ranging from mass sensors, signal processing, energy harvesting, up to health monitoring, laser scanners and bioengineering.

Kumar and Rhoads investigate an optically actuated bistable MEMS device [3], Hornstein and Gottlieb multimode dynamics and internal resonances in non-contact atomic force microscopy [4], Cho *et al.* nonlinear hardening and softening response and the switching among them [5], Welte et al. parametric resonance and anti-resonance [6], Kacem *et al.* primary and superharmonic resonances [7], Tusset *et al.* chaos control designs [8], Gerson *et al.* pull-in phenomenon in electrically actuated meso scale beams [9], Vyasarayani *et al.* past pull-in behavior [10], Ouakad and Ramini *et al.* response to mechanical shock [11, 12], Arlett *et al.* and Eom *et al.* extensively review current advances in nanotechnologies and their related applications in chemical/biological sensing and detection [13, 14], Villanueva *et al.*, Belardinelli *et al.*, and Corigliano *et al.* address the problem of design and reliability assessment [15-17], Kozinsky *et al.* describe the effect of disturbances in the experimental initial conditions [18], etc.

Motivated by the increasing relevance of nonlinear features, the present research study analyzes a theoretical bistable MEMS device, Fig. 1. A considerable versatility of behavior is observed, since the disappearance of the attractors may eventually lead either to jump and hysteresis loops with both small and large oscillation amplitudes, or, alternatively, to dynamic pull-in. In particular, we investigate the nonlinear response when, starting from the initial condition of rest, the device is subjected to a suddenly applied electrodynamic excitation.

Extensive numerical simulations are performed. Special attention is dedicated to the presence of disturbances. As previously observed in Thompson and coworkers [19, 20], disturbances are inevitably encountered under realistic conditions. They produce small, but finite perturbations, which may significantly affect and alter the system response. Taking them into

account is essential for reliable safety estimation of systems load carrying capacity. To this purpose, we need to overcome the merely local perspective and investigate the global one, where the overall dynamic behavior is explored. This fundamental issue is recently reviewed and reconsidered in Lenci and Rega [21, 22], where all the basic aspects are illustrated and discussed, including the difference with respect to the classical stability concepts, the main current advances in analytical tools for quantifying the integrity of a system against disturbances, and the actual substantial developments in the direction of practical applications. Dynamical integrity predictions have been recently widely referred in the literature in micro and nanosystems, both for interpreting and predicting the experimental behavior [23, 24], and for getting hints towards engineering design [25, 26], and for controlling the global dynamics [27].

In this framework, we perform a dynamical integrity analysis of the MEMS dynamical response to sudden excitations. Our aim is to develop an applicable confident estimate of the MEMS nonlinear behavior, which is essential for proper design, performance analysis, and calibration. The outline of the paper is as follows. The MEMS device is introduced (section 2), some preliminary investigations are performed (section 3), dynamical integrity charts are drawn (section 4), and the main conclusions are summarized (section 5).

2 The MEMS device

The analyzed MEMS device is represented in Fig. 1. The authors previously considered this microstructure in [25], where a simple single mode reduced order model was derived and extensive theoretical simulations were performed. In this section we briefly recall the major results, since they represent the starting point of the present paper.

The device consists of a slender imperfect microbeam, which is actuated by an electrostatic voltage load V_{DC} and an electrodynamic harmonic load of amplitude V_{AC} and frequency Ω. The microbeam has length l and a constant rectangular cross section of width b and thickness h. The shallow arched initial shape, which simulates the imperfections possibly due to the microfabrication process is expressed by $y_0(z) = (1/2)\, y_0(1-\cos(2\pi z))$, where y_0 is the maximum initial rise. The microbeam is subjected to a constant axial load P, which produces the axial displacement w_B at the right end B. Assuming l = 400 μm, h = 1.4 μm, b = 25μm, d = 2.2 μm, y_0 = 0.1 μm, n = 60 (i.e. w_B = 25nm), V_{DC} = 1.2V, the single-mode reduced order model is:

$$\ddot{Y} + 0.17247\,\dot{Y} - 0.325217 - 256.704\,Y - 445.54\,Y^2 + 2866.89\,Y^3 + (1.2 + V_{AC}\cos(\Omega t))^2 \cdot (0.016816 + 0.12395\,Y + 0.35318\,Y^2 + 0.46159\,Y^3 + 0.233094\,Y^4)/(1.44\,(0.596+Y)^6) = 0 \quad (6)$$

The system has a double potential well, with escape direction. Accordingly, the device may exhibit a bistable static behavior, i.e. at rest has two stable equilibrium configurations, an upper one and a lower one.

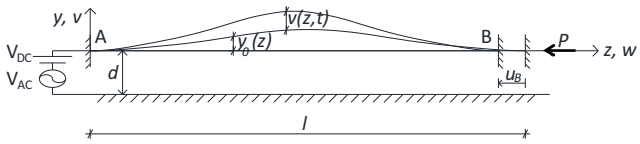

Fig. 1. A schematic model of the MEMS device.

Thanks to the inherent nonlinearities, the dynamics of the analyzed MEMS device are particularly rich, which is due to the coexistence of several principal competing attractors with different characteristics. This leads to a considerable versatility of behavior. The frequency response diagram in Fig. 2 shows both in-well oscillations belonging both to the principal well (denoted by A), and to the secondary well (denoted by B), and large cross-well oscillations. Both A and B exhibit both non-resonant and resonant branch, which undergo softening behavior, with the characteristic bending toward lower frequencies.

3 Theoretical final behavior at suddenly applied electrodynamic excitation

We consider the initial condition of rest in the left well, and analyze the trajectory when the electric excitation is suddenly applied. Our aim is to understand both if there will be a bounded motion or dynamic pull-in, and, in case of bounded motion, to distinguish which one of those detected in Fig. 2 will appear. The overall scenario is summarized in Fig. 3. It describes the final outcome that will theoretically occur when a certain V_{AC} and a certain Ω are suddenly applied. Green, orange and white respectively denote oscillations in the left well, oscillations in the right well, and escape.

A large compact green area exists, which denotes that there is a wide parameter range where a suddenly applied excitation from the rest configuration in the left well produces oscillations in the same well. A fall in the green area occurs at Ω = 18 (in the left neighbourhood of the resonance frequency), where a large V-shaped orange fractal area is observed. As far as the voltage is kept low, only bounded motions occur. Increasing the voltage, instead, fractal tongues involve the escape.

In practice disturbances exist, which are not considered in these simulations. As experimentally observed by the authors in previous studies [23, 24], they may alter the final outcome, making it different from the theoretical predictions. To take disturbances into account, we develop a dynamical integrity analysis.

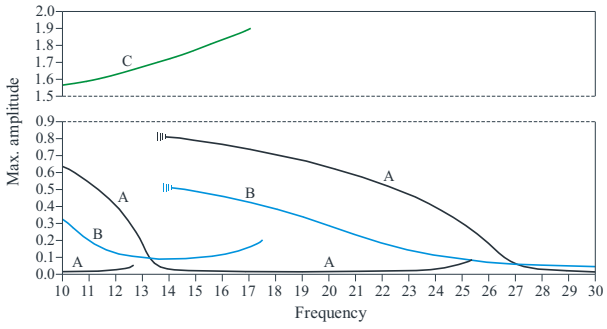

Fig. 2. Frequency response at V_{AC} = 3.5V.

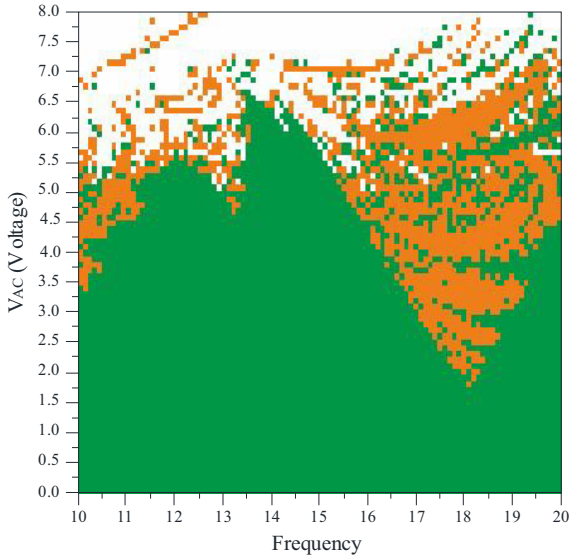

Fig. 3. Behavior chart for initial condition of rest in left well.

4 Practical final behavior at suddenly applied electrodynamic excitation

We focus on the range in Fig. 3 where a bounded motion is expected. Our aim is to improve the analysis in order to detect which final attractor will be caught in practice.

Taking into account the presence of disturbances requires analyzing the system behavior not only locally, by studying the response of each single initial condition of rest to sudden electric excitation, but also globally, by focusing on the attractor-basin scenario. An example of attractor-basin phase portrait is reported in Fig. 4. Green, red and orange denote the basins of the non-resonant B, the resonant B and the non-resonant A, respectively. The dark red dots mark each initial condition of rest. To guarantee that the analyzed initial condition of rest leads to a certain attractor, it is essential that this initial condition is surrounded by its basin. A large compact area of this basin is necessary to tolerate disturbances. Conversely, a small area is sensitive to perturbations, i.e. the final outcome may be different in practice from the theoretical predictions.

We consider as safe basin the basin of attraction of each single attractor. To measure the dynamical integrity, we introduce the Extended Local Integrity Measure (ELIM), which extends the definition of LIM introduced by Soliman and Thompson in [20], in order to consider initial conditions different from each single attractor. In particular, ELIM may be defined as the normalized radius of the largest circle entirely belonging to the safe basin and centered at the initial condition under consideration. Examples of circles used in the definition of ELIM are reported in Fig. 4. We normalize each radius with the analogous radius drawn for the initial condition of rest in the right well in the unforced dynamics.

An example of ELIM integrity profile is reported in Fig. 5, which describes ELIM dynamical integrity vs frequency, at certain fixed V_{AC} voltage. Where ELIM has elevated values, e.g. ELIM > 10%, the initial condition of rest is expected to lead not only in theory but also in practice to the particular attractor predicted in Fig. 3.

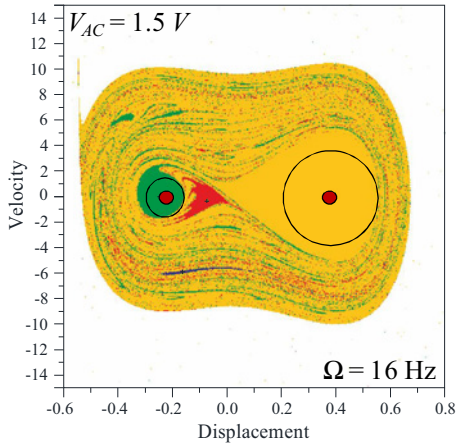

Fig. 4. Attractor-basin phase portrait at $\Omega = 16$, $V_{AC} = 1.5V$. Initial conditions of rest in the left and right well are in red dots. Examples of circles used in ELIM definition are in solid line.

Where ELIM drops to smaller values, the attractor theoretically expected to exist may practically disappear under realistic conditions, i.e. in the parameter ranges where ELIM becomes too small, a different bounded attractor may appear in practice.

Collecting information from several integrity profiles at different values of V_{AC}, we build the ELIM integrity chart, which shows the curves of constant percentage of ELIM, Fig. 6. For convenience, they are overlapped to the results obtained in Fig. 3 (shown in grayscale). The curves describe the overall scenario of structural safety of the initial condition of rest when subjected to a suddenly applied excitation of different frequency and voltage.

The curves are nearly parallel to the boundaries of the green (dark grey) compact area. At low voltage, elevated ELIM is guaranteed, i.e. when the device is excited from the rest position, attractor B can be safely observed. At high voltage, small ELIM occurs, i.e. attractor B (even if theoretically expected) may not appear in practice, but the device may exhibit another final motion (pull-in or another bounded attractor). The curves appear at about constant steps, i.e. the deterioration (or the increment) of the dynamical integrity is rather slow. This means that the range where the initial condition of rest in the left well practically leads to a safe attractor in the same well enlarges (reduces) significantly by decreasing (increasing) disturbances. A drop in ELIM dynamical integrity is observed at the V-shaped region, where the final outcome is very sensitive to disturbances despite the low voltage loads.

A similar analysis can be performed for the initial condition in the right well.

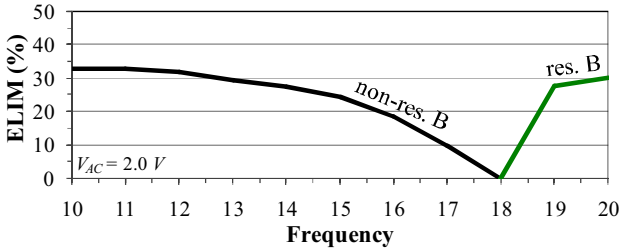

Fig. 5. ELIM integrity profiles for the initial condition of rest in the left well, at $V_{AC} = 2.0$ V.

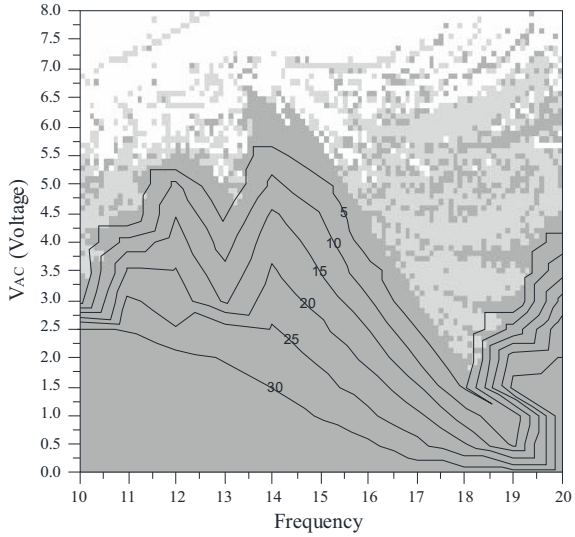

Fig. 6. ELIM integrity chart for the initial condition of rest in the left well.

The integrity curves may be used in the design to detect a lower bound of safety below which a certain final response may practically vanish, i.e. they point out that we cannot operate the MEMS device in safe conditions in the practical area where the initial condition of rest is not sufficiently robust (e.g. ELIM < 10%). It is concluded that the practical region of existence of a certain response is a subset of the theoretical one.

5 Conclusions

An electrically actuated MEMS device with considerable versatility of behavior has been analyzed. The device has a bistable static configuration, with possibility of escape. Systematic theoretical investigations have been performed to explore the nonlinear response when the device, from rest, is subjected to a suddenly applied electric excitation.

To take into account the inevitable presence of disturbances, a dynamical integrity analysis is carried out, where we have focused on the practical vulnerability of each attractor. ELIM integrity charts highlight that we cannot rely on the theoretical range of existence of each attractor, since disturbances considerably reduce the safe parameter range. The practical safe area is smaller, and sometimes remarkably smaller, than theoretical one.

We have emphasised that the integrity charts may be applied in the design to identify lower bounds of safety where we can operate the device with the desired motion in safe conditions. While we refer to a particular case-study, the approach is very general.

Acknowledgments

Laura Ruzziconi and Stefano Lenci acknowledge financial support by the Italian Ministry of Education, Universities and Research (MIUR) by the PRIN funded program 2010/11, grant N. 2010MBJK5B "Dynamics, stability and control of flexible structures".
Mohammad I. Younis acknowledges financial support by National Science Foundation through grant # 0846775.

References

1. S. D. Senturia, *Microsystem Design*, Kluwer Academic Publishers, Dordrecht (2001)
2. M. I. Younis, *MEMS Linear and Nonlinear Statics and Dynamics*, Springer (2011)
3. V. Kumar, J. F. Rhoads, J. Comput. Nonlinear Dynam. **7**:021007 (2012)
4. S. Hornstein, O. Gottlieb, J. Appl. Phys. **112**(7): 074314 (2012)
5. H. Cho, B. Jeong, M.F. Yu, A.F. Vakakis, D.M. McFarland, L.A. Bergman, Int. J. Solids Struct. **49**(15):2059-2065 (2012).
6. J. Welte, T.J. Kniffka, H. Ecker, Shock Vib. **20**(6): 1113-1124 (2013).
7. N. Kacem, S. Baguet, R. Dufour, S. Hentz, Appl. Phys. Lett. **98**, 193507 (2011).
8. Tusset A.M., Balthazar J.M., Bassinello D.G., Pontes JrBR,Felix JLP. Nonlinear Dyn. **69**:1837-1857 (2012)
9. Y. Gerson, I. Sokolov, T. Nachmias, B.R. Ilic, S. Lulinsky, S. Krylov, Sensors Actuators A: Physical **199**:227–235 (2013)
10. C.P. Vyasarayani, E. M. Abdel-Rahman, J. McPhee, S. Birkett, J. Comput. Nonlinear Dynam. **6**:031008 (2011)
11. H. M. Ouakad, J. Vib. Control doi: 10.1177/1077546313514763 (2013)
12. A. H. Ramini, M.I. Younis, Q.T. Su, Smart Mater. Struct. **22** (2), 025006 (2013)
13. J.L. Arlett, E.B. Myers, M.L. Roukes, Nature Nanotech. **6**:203-215 (2011)
14. K. Eom, H. S. Park, D. S. Yoon, T. Kwon, Physics Reports **503**:115–163 (2011)
15. L.G. Villanueva, R.B. Karabalin, M.H. Matheny, D. Chi, J.E. Sader, M.L. Roukes, Phys. Rev. B **87**(2), 024304 (2013).
16. P. Belardinelli, S. Lenci, M. Brocchini, J. Comput. Nonlinear Dynam (in press).
17. A. Corigliano, M. Dossi, S. Mariani, Computers Struct. **122**:113–127 (2013)
18. I. Kozinsky, H.W.C. Postma, O. Kogan, A. Husain, M.L. Roukes, Phys. Rev. Lett. **99**:207201 (2007).
19. J.M.T. Thompson, Proc. R. Soc. Lond. Ser. A **421**:195–225 (1989).
20. M.S. Soliman, J.M.T. Thompson, J. Sound Vib. **135**:453–475 (1989).
21. S. Lenci, G. Rega, Int. J. Non-Linear Mech. **46**:1232–1239 (2011).
22. S. Lenci, G. Rega, Int. J. Non-Linear Mech. **46**:1240–1251 (2011).
23. L. Ruzziconi, M. I. Younis, S. Lenci, *IUTAM Symposium on Nonlinear Dynamics for Advanced Technologies and Engineering Design*, Wiercigroch, M., Rega, G. (eds.), **32**:249-261, Springer (2013).
24. L. Ruzziconi, M. I. Younis, S. Lenci, Meccanica, **48**(7): 1761-1775 (2013).
25. L. Ruzziconi, S. Lenci, M. I. Younis, Int. J. Bif. Chaos **23**(2):1350026 (2013).
26. G. Rega, V. Settimi, Nonlinear Dyn. **73**:101-123 (2013).
27. S. Lenci, G. Rega, J.Micromech. Microeng. **16**:390–401 (2006).